Contents lists available at ScienceDirect

Physics Letters B

www.elsevier.com/locate/physletb

Heavy neutrinos and the $pp \to lljj$ CMS data ☆

Janusz Gluza, Tomasz Jeliński *

Institute of Physics, University of Silesia, Uniwersytecka 4, 40-007 Katowice, Poland

A B S T R A C T

We show that the excess in the $pp \to eejj$ CMS data can be naturally interpreted within the Minimal Left–Right Symmetric model (MLRSM), keeping $g_L = g_R$, if CP phases and non-degenerate masses of heavy neutrinos are taken into account. As an additional benefit, a natural interpretation of the reported ratio (14 : 1) of the opposite-sign (OS) $pp \to l^{\pm}l^{\mp} jj$ to the same-sign (SS) $pp \to l^{\pm}l^{\pm} jj$ lepton signals is possible. Finally, a suppression of muon pairs with respect to electron pairs in the $pp \to lljj$ data is obtained, in accordance with experimental data. If the excess in the CMS data survives in the future, it would be a first clear hint towards presence of heavy neutrinos in right-handed charged currents with specific CP phases, mixing angles and masses, which will have far reaching consequences for particle physics directions.

1. Introduction

LHC is a perfect laboratory to test the Beyond Standard Model (BSM) scenarios. Recently, the CMS Collaboration announced an interesting excess in data, see point B in Fig. 1. This point is related to the process $pp \to eejj$ collected by $\sqrt{s} = 8$ TeV LHC corresponding to an integrated luminosity 19.7 fb^{-1} [1]. Several analyses [2–5] showed that this excess can be interpreted as a signal of charged gauge boson $W_2^{\pm}$ with mass about 2.2 TeV in the Left–Right symmetric model [6–8]. It is possible when gauge couplings connected with left and right $SU(2)$ groups are not equal to each other. For a case $g_L = g_R$ see point A in Fig. 1 (the measured cross section is suppressed by a factor of $\gamma_{CMS} = 0.23$ when compared with scenario in which $g_L = g_R$). Moreover, the number of events with same-sign (SS) leptons to the number of events with opposite-sign (OS) leptons is

$$r = \frac{N_{SS}}{N_{OS}} = \frac{1}{14}, \qquad (1)$$

and, finally, no excess in $\mu\mu$ channel has been reported [1,9].

Theoretical analyses of the left–right symmetric models speeded up considerably in recent years [10–32], after the LHC has started its operation. It is not surprising as this collider is operating at highest available so far energies, which means that new states of matter or new interactions can be probed more effectively. For instance, the left–right symmetric models offer an elegant, dynamical explanation for suppression of right-handed currents at low energies, and it might be that finally LHC can see them directly in experimental data analyses.[1]

Discovery of right-handed currents and new elementary states of matter in form of a charged heavy gauge boson and heavy neutrinos would be of paramount importance for our understanding of Physics in microscale. It would also impact Physics in macroscale. For instance, details of leptogenesis depend on CP phases of decaying particles, or Big Bang Nucleosynthesis and the dark matter problem raise questions about the matter content of the Universe [34,35] (neutrinos may be responsible for the matter-dominated flat Universe in which we live).

It is natural that experimental data analysis employs simplifications of theoretical models which quite often, thinking in terms of BSM, are much more complicated than the worthy Standard Model theory. However, in this way conclusions can be distorted or even some interesting and natural scenarios can be overlooked. We think that our discussion here is a good and important example showing that including some additional theoretical issues into analysis can finally pay back in terms of better understanding of experimental results.

In this paper, we show how including details of heavy neutrinos mass spectrum, their CP phases and non-trivial mixing matrix can change a picture, leading to natural interpretation of the data

---

[1] For other relevant arguments in favor of left–right symmetry, see e.g. [33].
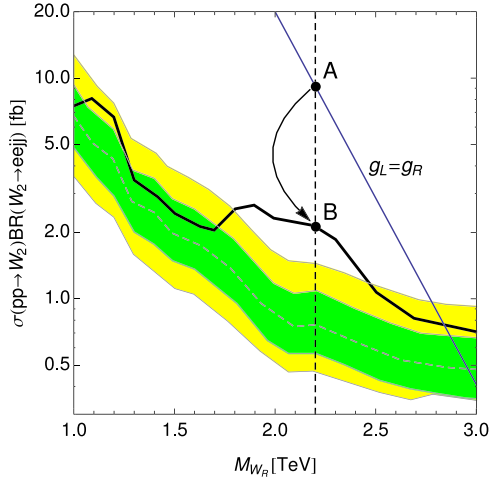
Fig. 1. CMS data for production of the first generation leptons with two jets in pp collision with $\sqrt{s} = 8$ TeV [1]. Blue solid line shows the CMS estimation of the cross section in the MLRSM model with $g_L = g_R$, diagonal heavy neutrino couplings and $M_N = M_{W_2}/2$. Explaining excess in the data around $M_{W_2} \sim 2.2$ TeV (point B) requires refinement of those assumptions (point A). (For interpretation of the references to colour in this figure legend, the reader is referred to the web version of this article.)

within the MLRSM, with $g_L = g_R$ and relatively light $W_2^{\pm}$ charged gauge boson mass.[2] In other words, we can get down from point A to point B in Fig. 1, while holding $g_L = g_R$. We can also accommodate value of r in (1) and explain a shortage of muon pairs.

We shall consider production of W_2 which further decays to a charged lepton l_i ($i = 1, 2, 3$) and an on-shell heavy neutrino N_a ($a = 1, 2, 3$) [36]. The latter further decays mainly via 3-body process $N_a \rightarrow l_j jj$ leading to two jets and two charged leptons in the final state:

$$pp \rightarrow W_2^{\pm} \rightarrow l_i^{\pm} N_a \rightarrow l_i^{\pm} l_j^{\mp} jj, \quad \text{(OS)} \tag{2}$$

$$pp \rightarrow W_2^{\pm} \rightarrow l_i^{\pm} N_a \rightarrow l_i^{\pm} l_j^{\pm} jj. \quad \text{(SS)} \tag{3}$$

We have left considering distributions of kinematical variables of leptons and jets as well as cuts issue in the discussed processes for future studies.

2. Heavy neutrino interactions and their CP parities

We work within the MLRSM model in which $g_L = g_R$, $v_L = 0$ and $\kappa_2 = 0$ (what results in no $W_L - W_R$ mixing). The scale of breaking $SU(2)_R$ is set to $v_R = 4.77$ TeV, such that the mass of W_2 is about 2.2 TeV (see Fig. 1). Moreover, to simplify our considerations, let us assume that the scalar potential parameters are chosen such that all scalar particles beside the lightest Higgs boson have masses of order v_R. We leave discussion of their influence on $pp \rightarrow lljj$ for future studies.

Neutrino mass matrix is chosen to be of the form

$$M_\nu = \begin{pmatrix} 0 & M_D \\ M_D^T & M_R \end{pmatrix}. \tag{4}$$

---

[2] In this work, we do not discuss which scenarios are more natural, those with $g_L = g_R$, or those without it. If we demand strict unification of gauge couplings then scenarios with $g_L \neq g_R$ seem to be more appropriate [2–4]. However, also such models need additional modifications, like new intermediate scales or symmetries. This problem is not of the main importance for our work, and we shall remain with the simplest possibility, which is $g_L = g_R$. The MLRSM has an additional advantage as $g_L = g_R$ preserves P symmetry and simplifies model parameters, e.g. gauge bosons mass relations.

Typically, Dirac masses M_D are much smaller than Majorana masses M_R i.e. $M_D \ll M_R$, e.g. $M_D \sim 10^{-3}$ GeV, $M_R \sim 10^3$ GeV. Hence light neutrinos $\nu_{1,2,3}$ obtain masses $M_{\nu_{1,2,3}}$ of the order of 1 eV via type I see-saw mechanism. Unitary matrix U which enters Takagi decomposition $M_\nu = U^T \text{diag}(M_{\nu_1}, M_{\nu_2}, M_{\nu_3}, M_{N_1}, M_{N_2}, M_{N_3})U^\dagger$ is of the following form:

$$U \approx \begin{pmatrix} 1 & 0 \\ 0 & K_R^\dagger \end{pmatrix}, \tag{5}$$

where, K_R is an unitary 3×3 matrix defined by $M_R = K_R^T \text{diag}(M_{N_1}, M_{N_2}, M_{N_3})K_R$, $M_{N_a} > 0$. For simplicity, we assume no light-heavy neutrino mixings (they are negligible or very small [37]). Such choice of U means that $W_2^{\pm}$ does not couple to light neutrinos ν_a, and heavy neutrinos N_a do not couple to $W_1^{\pm}$. Exact neutrino mixing matrix U can also be considered, which include non-zero off-diagonal light-heavy matrix elements in (5) [19].

K_R matrix enters directly heavy neutrinos – W_2 interactions, which can be cast in the following form [38]:

$$\mathcal{L} \supset \frac{g_L}{\sqrt{2}} \overline{N}_a \gamma^\mu P_R (K_R)_{aj} l_j W_{2\mu}^+ + \text{h.c.} \tag{6}$$

In general elements of the K_R matrix can be complex. In a CP-conserving case, CP parities of heavy neutrinos are purely imaginary [39,40] and, in fact, they can be connected with elements of the K_R matrix. In practice, if CP parities of all three heavy neutrinos are the same, $\eta_{CP}(N_1) = \eta_{CP}(N_2) = \eta_{CP}(N_3) = +i$, then elements of the K_R matrix can all be made real. If, for instance, $\eta_{CP}(N_1) = \eta_{CP}(N_2) = -\eta_{CP}(N_3) = +i$ then K_{Ri3} element is complex. Choosing different scenarios have far-reaching consequences in phenomenological studies. Let us consider processes where heavy neutrinos propagate as virtual states, then their contributions to the amplitudes must be summed over. In general, constructive or destructive interferences between heavy neutrinos can appear. For instance, in the neutrinoless double beta decay $(\beta\beta)_{0\nu}$ process, or its inverse collider version process $e^- e^- \rightarrow W^- W^-$, amplitudes include squared matrix elements $(K_R)_{1a}^2$. If all heavy neutrinos have the same CP parities, then elements of the K_R matrix can all be made real, and all heavy neutrinos contribute constructively into the amplitudes, otherwise destructive interferences can appear. Such scenarios have been considered in full details in phenomenological analyses in [41]. It has been shown there that cancellations among contributions to the amplitude from heavy neutrinos with opposite CP parities can appear. In this way, low energy $(\beta\beta)_{0\nu}$ constraints can be avoided and for instance the collider signal $e^- e^- \rightarrow W^- W^-$ can be substantial. We will see in the next Section that CP phases of heavy neutrinos play a crucial role also in a case of SS and OS $pp \rightarrow lljj$ signals.

3. Cross sections

We shall show that interference effects, CP phases of heavy neutrinos and their mass splittings are relevant for the prediction of the $pp \rightarrow lljj$ cross section. To expose interference effects in a clear way, the following three different setups will be discussed: (A) neutrinos have degenerate masses, (B) one neutrino is lighter than W_2, (C) two neutrinos are lighter than W_2, and, (D) finally, there is only small mass splitting among neutrinos. The numerical analysis has been done with the help of MADGRAPH5 (v2.2.2) [42] and with our implementation of the MLRSM in FEYNRULES (v2.0.31) [43,44].

To simplify notation we shall denote cross-sections for the process $pp \rightarrow l_i^{\pm} l_j^{\mp} jj$ by $\sigma_{l_i l_j}^{\pm\mp}$ etc. For reference points it is assumed, as in CMS [1] analysis, that $M_N = M_{W_2}/2$ with diagonal and real K_R

mixing matrix in (6), which for $\sqrt{s} = 8$ TeV and $M_{W_2} = 2.2$ TeV, gives:

$$\sigma(pp \to W_2^{\pm}) = \begin{cases} 71.16 \text{ fb}, \\ 21.09 \text{ fb}, \end{cases} \qquad (7)$$

what agrees with recent estimations on $pp \to W_2 \to jj$ cross section [45]. For chosen value of v_R and diagonal matrix K_R relevant branching ratios are:

$$\text{BR}(W_2^{\pm} \to e^{\pm} N_a) = 0.058, \qquad (8)$$

$$\text{BR}(N_a \to e^{\pm} jj) = 0.35 \qquad (9)$$

when all heavy neutrinos have the same mass $M_N = M_{W_2}/2$, and

$$\text{BR}(W_2^{\pm} \to e^{\pm} N_1) = 0.066 \qquad (10)$$

when only $M_{N_1} = M_{W_2}/2$ while $N_{2,3}$ are heavier than W_2.

3.1. Degenerate masses of heavy neutrinos

First, let us examine the following mass pattern in which all heavy neutrinos are degenerate and lighter than W_2:

$$M_N := M_{N_a} = M_{W_2}/2. \qquad (11)$$

In this setup, and also for small mass differences between heavy neutrinos, the narrow width approximation (NWA) will not work because of the interference effects.

Let us take K_R in the following form (which is in fact a product of real, orthogonal transformation and diagonal phase matrix)

$$K_R = \begin{pmatrix} \cos\theta_{12} & \sin\theta_{12} & 0 \\ -e^{i\phi_2}\sin\theta_{12} & e^{i\phi_2}\cos\theta_{12} & 0 \\ 0 & 0 & 1 \end{pmatrix}. \qquad (12)$$

This is a simplified version of a complete unitary rotation matrix [46].

In this way, we assume mixings between two lepton flavours only. Phase ϕ_2 is connected with CP parity of heavy neutrinos $N_{1,2}$, CP-conserving case is realized when $\phi_2 = 0, \pm\pi/2, \pm\pi$. All phases which do not fulfil the above relations break CP symmetry. In general, in the MLRSM with the mass matrix of the form (4) we have six CP phases; if $v_L \neq 0$ ($M_L \neq 0$) then there are 18 CP phases [47].

Using this simple form of the matrix K_R we are already able to discuss all relevant effects connected with mixings and CP phases in the considered process.

First, in the case of degenerate neutrinos, $\sigma_{l_i l_j}^{\pm\mp}$ with $i = j$ does not depend on mixing angles at all, and is zero for $i \neq j$:

$$\sigma_{l_i l_j}^{\pm\mp} = \frac{g_L^4}{4} \left| \sum_a F^{\pm\mp}(s, M_{W_2}^2, M_N^2)(K_R^{\dagger})_{ia}(K_R)_{aj} \right|^2$$

$$= \delta_{ij} \frac{g_L^4}{4} F^{\pm\mp}(s, M_{W_2}^2, M_N^2) = \delta_{ij} \widehat{\sigma}_{SF}^{\pm\mp}, \qquad (13)$$

where the second equality comes from the unitarity of the K_R, while the third defines $\widehat{\sigma}_{SF}^{\pm\mp}$. $F^{\pm\mp}$ is a function of center of mass energy $\sqrt{s}$ and masses M_{W_2} and M_N (leptons and constituents of jets are treated as massless). From now on we will not write down arguments of the F functions.

On the other hand, for same-sign signature i.e. l^+l^+ or l^-l^- the mixing matrix K_R does not cancel from the cross section formula:

$$\sigma_{l_i l_j}^{\pm\pm} = \frac{g_L^4}{4} \left[F_1^{\pm\pm} + (-1)^{\delta_{ij}} F_2^{\pm\pm} \right]$$

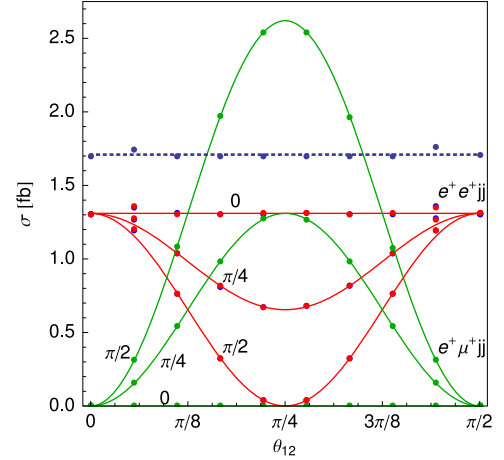$$\times \left| \sum_a (K_R^{\dagger})_{ia}(K_R^*)_{aj} \right|^2. \qquad (14)$$

Fig. 2. Cross section $pp \to lljj$ for the production of two SS light leptons with two jets jj for $\phi_2 = 0$, $\pi/4$ and $\pi/2$: e^+e^+ (red), $\mu^+\mu^+$ (red, same as for e^+e^+) and $e^+\mu^+$ (green). Plots for σ^{--} are of the same shape but with $\widehat{\sigma}_{SF}^{++}$ changed by $\widehat{\sigma}_{SF}^{--}$ in (15). Solid lines show formulas (15), while green and red dots are numerical results obtained in MADGRAPH5. The blue dotted line shows corresponding cross section for the OS process $pp \to W_2^{\pm} \to e^+e^- jj$, which is independent of θ_{12} – see (13). (For interpretation of the references to colour in this figure legend, the reader is referred to the web version of this article.)

As a consequence, cross section for $l_i^{\pm}l_j^{\pm}$ with $i = j$ is correlated with that for which $i \neq j$ i.e.

$$\sigma_{l_i l_j}^{\pm\pm} = \begin{cases} \widehat{\sigma}_{SF}^{\pm\pm}(1 - \sin^2 2\theta_{12}\sin^2\phi_2) & \text{for } i = j, \\ \widehat{\sigma}_{DF}^{\pm\pm}\sin^2 2\theta_{12}\sin^2\phi_2 & \text{for } i \neq j, \end{cases} \qquad (15)$$

where $\widehat{\sigma}_{SF}^{\pm\pm}$ and $\widehat{\sigma}_{DF}^{\pm\pm}$ correspond to maximal values of cross sections for same-flavour (SF) and different flavour (DF) cases. For the numerical results see Fig. 2. The difference in $\widehat{\sigma}_{DF}^{\pm\pm}$ and $\widehat{\sigma}_{SF}^{\pm\pm}$ is related to the standard factor of (-1) appearing in same-flavour Feynman diagrams. For $\sqrt{s} = 8$ TeV and $M_N = 1.1$ TeV they read $\widehat{\sigma}_{SF}^{++} = 1.31$ fb, $\widehat{\sigma}_{SF}^{--} = 0.39$ fb, $\widehat{\sigma}_{DF}^{++} = 2.61$ fb, $\widehat{\sigma}_{DF}^{--} = 0.78$ fb and $\widehat{\sigma}_{SF}^{\pm\mp} = 1.70$ fb. $\widehat{\sigma}^{--}$ is about 3.4 times smaller than $\widehat{\sigma}^{++}$ due to asymmetry in production of $W_2^{\pm}$, see (7).

As one can see from (15) and Fig. 2, there exists a CP phase for which $(\sigma_{ee}^{++} + \sigma_{ee}^{--})/\sigma_{ee}^{+-} = r$ as suggested by CMS data (1). Namely, that relation holds when θ_{12} and ϕ satisfy

$$\sin^2 2\theta_{12}\sin^2\phi_2 = 1 - \frac{r}{c}, \qquad (16)$$

where $c = (\widehat{\sigma}_{SF}^{++} + \widehat{\sigma}_{SF}^{--})/\widehat{\sigma}_{SF}^{+-} \approx 1$. As a consequence same-sign different-flavour cross section is $\sigma_{e\mu}^{\pm\pm} = \widehat{\sigma}_{DF}^{\pm\pm}(1 - r/c)$. Moreover the total cross section for $pp \to eejj$ is then

$$\sigma_{ee}^{(\text{tot})} = \widehat{\sigma}_{SF}^{\pm\mp}[1 + 1 + c - c\sin^2 2\theta_{12}\sin^2\phi_2]. \qquad (17)$$

One can check that the total cross section $\sigma_{ee}^{(\text{tot})}$ is suppressed by a factor

$$\gamma = \frac{1+r}{1+c} \approx 0.54 \qquad (18)$$

with respect to $\theta_{12} = \phi_2 = 0$ case ($\sigma_{ee}^{(\text{tot},0)}$). Our numerical calculations yield $\sigma_{ee}^{(\text{tot},0)} = 3.41$ fb. Hence when θ_{12} and ϕ_2 are chosen such that (16) is satisfied then

$$\sigma_{ee}^{(\text{tot})} = \gamma\sigma_{ee}^{(\text{tot},0)} = 1.84 \text{ fb} \qquad (19)$$

what is about 81% of the excess reported by the CMS (point B in Fig. 1). Moreover, in consequence of (15) total cross section for production of two muons with two jets is the same as for electrons:

$\sigma_{ee}^{(tot)} = \sigma_{\mu\mu}^{(tot)}$. Hence the discussed scenario would also result in excess in $\sigma(pp \to \mu\mu jj)$. That is in contradiction with the CMS data related to $pp \to \mu\mu jj$ [1].

3.2. $M_{N_1} < M_{W_2} < M_{N_{2,3}}$

In this case only N_1 can be on-shell. We choose $M_{N_1} = 1.1$ TeV $= M_{W_2}/2$; the remaining two neutrinos are much heavier, $M_{N_{2,3}} = 10$ TeV.

Here one can use narrow width approximation (NWA) to estimate cross-section for $pp \to l_1 l_2 jj$ going through on-shell W_2, which decays to l_i and on-shell N_1 and the latter decays to $l_j jj$:

$$\sigma_{l_i l_j} = \sigma(pp \to W_2) \mathrm{BR}(W_2 \to l_i N_1)$$
$$\times \mathrm{BR}(N_1 \to l_j jj). \tag{20}$$

Since quarks and leptons masses are much smaller than the N_1 mass, 3-body decay of N_1 mediated by off-shell W_2 can be treated analogously to well-known muon decay in the Fermi theory. One can check that

$$\Gamma(N_a \to l_i^- q_\alpha \bar{q}_\beta) = \frac{g_L^4}{2048\pi^3} |(K_R)_{ai}^*|^2 |(U_{CKM}^R)_{\alpha\beta}|^2$$
$$\times M_{N_a} F(x_a), \tag{21}$$

where $x_a = M_{N_a}^2/M_{W_2}^2$ while the function

$$F(x) = \frac{12}{x} \left[1 - \frac{x}{2} - \frac{x^2}{6} + \frac{1-x}{x} \ln(1-x) \right] \tag{22}$$

encompasses full tree-level contribution from the W_2 propagator [48]. The presence of such a factor makes N_a decay width really sensitive to the ratio $x_a = M_{N_a}^2/M_{W_2}^2$, e.g. for fixed M_{W_2} it can be enhanced by a factor of ~ 27 when $M_{N_a} \approx M_{W_2}$ with respect to the scenario $M_{N_a} \approx M_{W_2}/2$.

Summing over all possible final states and taking into account the unitarity of K_R and U_{CKM}^R one obtains the total decay width of N_a

$$\Gamma(N_a) = \sum_{i,\alpha\beta} \left[\Gamma(N_a \to l_i^- q_\alpha \bar{q}_\beta) + \Gamma(N_a \to l_i^+ \bar{q}_\alpha q_\beta) \right]$$
$$= \frac{9g_L^4}{1024\pi^3} M_{N_a} F(x_a). \tag{23}$$

Hence the BRs under consideration are

$$\mathrm{BR}(N_a \to l_i^- q_\alpha \bar{q}_\beta) = \frac{1}{6} |(K_R)_{ai}^*|^2 |(U_{CKM}^R)_{\alpha\beta}|^2, \tag{24}$$

$$\mathrm{BR}(N_a \to l_i^+ \bar{q}_\alpha q_\beta) = \mathrm{BR}(N_a \to l_i^- q_\alpha \bar{q}_\beta). \tag{25}$$

Using assumed masses, we have scanned over $\theta_{12} \in \langle 0, \pi/2 \rangle$ to verify dependence of $\sigma_{l_i l_j}$ on that angle. The CP phase ϕ_2 was set to $\pi/2$ (CP-conserving case), i.e.

$$K_R = \begin{pmatrix} \cos\theta_{12} & \sin\theta_{12} & 0 \\ -i\sin\theta_{12} & i\cos\theta_{12} & 0 \\ 0 & 0 & 1 \end{pmatrix}. \tag{26}$$

The obtained dependences are shown in Figs. 3, 4 and 5. On these plots, we present contributions to the total cross section $\sigma_{l_i l_j}$ from subprocesses with different charges and flavours of leptons in the final state. The scale on the vertical axes is the same for all these plots to clearly show relative values of individual cross sections. The total cross section itself is shown in Fig. 6.

Let us first note that there is no interference between different contributions to $pp \to l_i^+ l_j^- jj$, see Fig. 3, because the corresponding initial states (at the parton level) are different. Secondly,
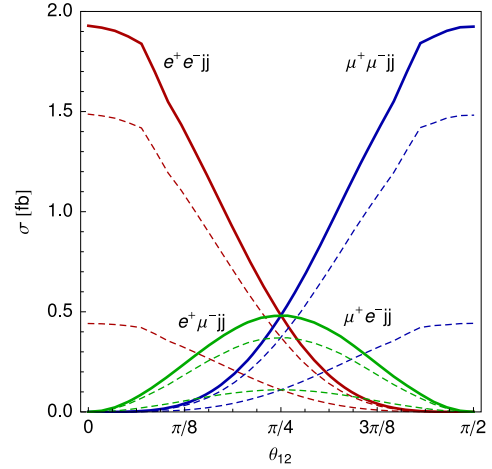

Fig. 3. Cross section σ for the production of two opposite-sign light leptons $l_i = e, \mu$ with two jets jj in the process $pp \to W_2^\pm \to l_i^+ l_i^- jj$ with $\sqrt{s} = 8$ TeV for $M_{N_1} = M_{W_2}/2$, $M_{N_{2,3}} > M_{W_2}$. The dashed lines display contributions from intermediate channels $W_2^\pm \to e^\pm N_1$ and $W_2^\pm \to \mu^\pm N_1$. Solid lines correspond to sum over possible channels.
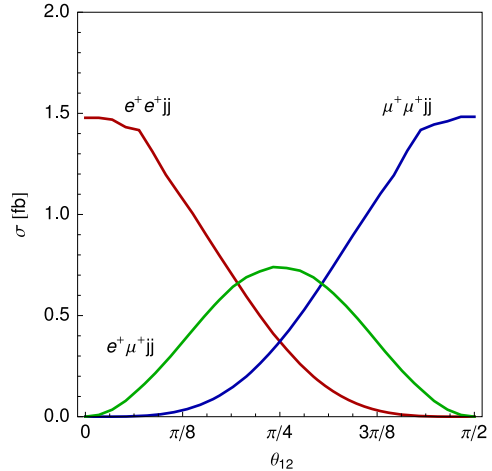

Fig. 4. Cross section σ for the production of two same-sign light leptons $l_i^+ = e^+, \mu^+$ with two jets jj in the process $pp \to W_2^+ \to l_i^+ l_j^+ jj$ with $\sqrt{s} = 8$ TeV for $M_{N_1} = M_{W_2}/2$, $M_{N_{2,3}} > M_{W_2}$.
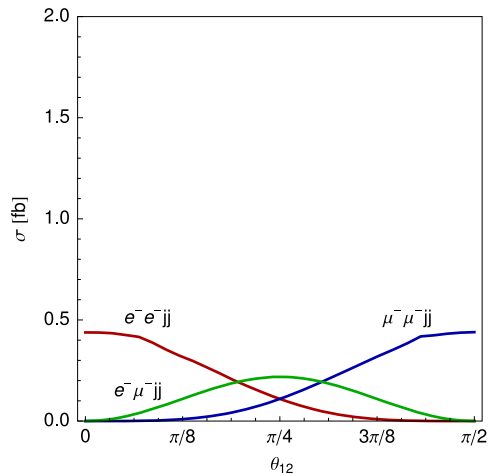

Fig. 5. Cross section σ for the production of two same-sign light leptons $l_i^- = e^-, \mu^-$ with two jets jj in the process $pp \to W_2^- \to l_i^- l_j^- jj$ with $\sqrt{s} = 8$ TeV for $M_{N_1} = M_{W_2}/2$, $M_{N_{2,3}} > M_{W_2}$.
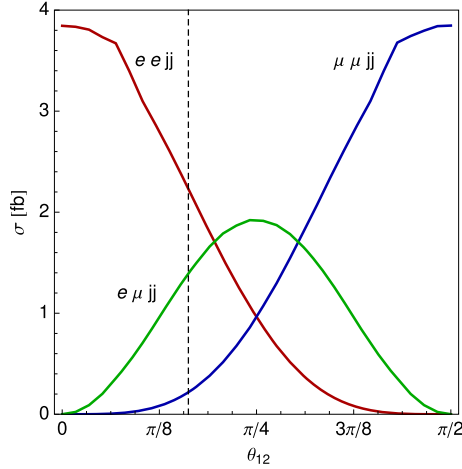
Fig. 6. The total cross section σ for the production of two light leptons $l_i = e, \mu$ with two jets jj in the process $pp \to W_2 \to l_i l_j jj$ with $\sqrt{s} = 8$ TeV for $M_{N_1} = M_{W_2}/2$, $M_{N_{2,3}} > M_{W_2}$. The vertical dashed line displays value of θ_{12} for which $\sigma_{ee}^{(tot)}$ (red solid line) matches the CMS excess value (point B in Fig. 1). (For interpretation of the references to colour in this figure legend, the reader is referred to the web version of this article.)

due to their large masses $N_{2,3}$ are decoupled and effectively only contributions from Feynman diagrams containing N_1 are relevant. In this case NWA can be used to understand qualitative dependence on the mixing angle θ_{12}. Namely, using (20) one obtains $\sigma_{ee} \sim \cos^4 \theta_{12}$, $\sigma_{\mu\mu} \sim \sin^4 \theta_{12}$ and for different-flavour signature $\sigma_{e\mu} \sim \sin^2 2\theta_{12}$, cf. Figs. 3, 4 and 5. Thirdly, one can check that, due to decoupling of $N_{2,3}$, in this setup CP phases do not influence cross sections because the interference between diagrams with different N_a is suppressed by large mass of $N_{2,3}$. It is worthwhile to note that here, as in Sec. A, the difference between maximal value of $\sigma_{ee}^{\pm\pm}$ and $\sigma_{e\mu}^{\pm\pm}$, see Figs. 4 and 5, comes from the standard factor of (-1) appearing in same-flavour Feynman diagrams. Finally, our numerical analysis shows that in this scenario $\sigma_{ee}^{(tot,0)} = 3.89$ fb hence to address CMS excess in $\sigma_{ee}^{(tot)}$ one has to adjust θ_{12} to 0.51. At the same time $\sigma_{\mu\mu}^{(tot)} = 0.21$ fb, see Fig. 6, so there is no excess in the $\mu\mu jj$ what is in accordance with CMS data [1,9]. However as one can check, cf. Figs. 4 and 5, sum of same-sign signature cross sections i.e. $\sigma_{ee}^{++} + \sigma_{ee}^{--}$ is nearly equal to σ_{ee}^{+-} for all values of mixing angle θ_{12}. As a consequence, in this setup $r \approx 1$ and one cannot address (1) by adjusting θ_{12}.

3.3. $M_{N_{1,3}} < M_{W_2} < M_{N_2}$

However, it turns out that one can arrange parameters of the models such that all above-mentioned experimental constraints are fulfilled. Namely, let us now consider the following mass pattern:

$$M_{N_{1,3}} = 0.925 \text{ TeV}, \quad M_{N_2} = 10 \text{ TeV} \tag{27}$$

and mixing matrix of the form:

$$K_R = \begin{pmatrix} \cos\theta_{13} & 0 & \sin\theta_{13} \\ 0 & 1 & 0 \\ -e^{i\phi_3}\sin\theta_{13} & 0 & e^{i\phi_3}\cos\theta_{13} \end{pmatrix}. \tag{28}$$

One expects that here $\mu\mu jj$ signal should be suppressed due to the large mass of N_2. In fact, it is confirmed by numerical computations: $\sigma_{\mu\mu}^{(tot,0)} \approx 0$ fb while $\sigma_{ee}^{(tot,0)} = 4.21$ fb. Because in this scenario N_1 and N_3 are degenerate in masses, one also gets: $\sigma_{\tau\tau}^{(tot)} = \sigma_{ee}^{(tot)}$. Let us note that here BR($W_2^\pm \to e^\pm N_{1,3}$) = 0.071 due to $x_{1,3} = M_{N_{1,3}}^2/M_{W_2}^2 \approx 0.18$ and $x_3 = M_{N_2}^2/M_{W_2}^2 > 1$, see Appendix A. That enhancement of BR with respect to (8) compensates
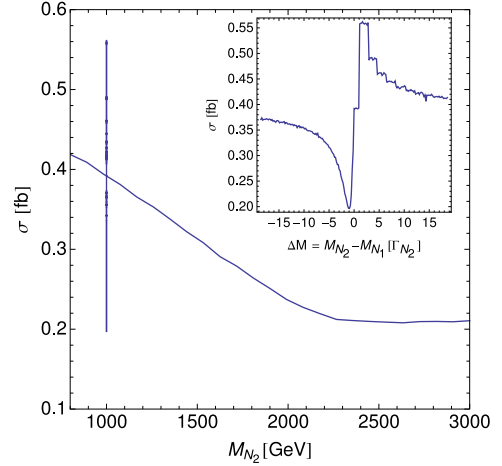

Fig. 7. Cross section $pp \to e^+ e^+ jj$ with $\theta_{12} = \phi = \pi/4$. Subplot in this figure exhibits interference effects for small splitting in masses of heavy neutrinos. Note that on the subplot mass difference $\Delta M = M_{N_2} - M_{N_1}$ is expressed in terms of multiplicities of N_2 decay width $\Gamma_{N_2} \approx 0.53 \times 10^{-3}$ GeV.

deficit in (19). As previously, analysis of contributions from heavy neutrinos $N_{1,3}$ gives $\sigma_{l_i l_j}^{\pm\mp} = \delta_{ij} \hat{\sigma}_{SF}^{\pm\mp}$ and:

$$\sigma_{l_i l_j}^{\pm\pm} = \begin{cases} \hat{\sigma}_{SF}^{\pm\pm}(1 - \sin^2 2\theta_{13} \sin^2 \phi_3) & \text{for } i = j, \\ \hat{\sigma}_{DF}^{\pm\pm} \sin^2 2\theta_{13} \sin^2 \phi_3 & \text{for } i \neq j, \end{cases} \tag{29}$$

where $i, j \in \{1, 3\}$. Now the maximal values of cross sections are: $\hat{\sigma}_{SF}^{\pm\mp} = 2.14$ fb, $\hat{\sigma}_{SF}^{++} = 1.63$ fb, $\hat{\sigma}_{SF}^{--} = 0.48$ fb and $\hat{\sigma}_{DF}^{++} = 3.27$ fb, $\hat{\sigma}_{DF}^{--} = 0.96$ fb. Moreover,

$$\sin^2 2\theta_{13} \sin^2 \phi_3 = 1 - \frac{r}{c} \tag{30}$$

has to be satisfied in order to ensure $r = 1/14$. As previously, $c = (\hat{\sigma}_{SF}^{++} + \hat{\sigma}_{SF}^{--})/\hat{\sigma}_{SF}^{+-} \approx 1$ and $\gamma \approx 0.54$ what gives $\sigma_{ee}^{(tot)} = \gamma \sigma_{ee}^{(tot,0)} = 2.27$ fb. It is precisely the value of $\sigma(pp \to eejj)$ reported by the CMS (point B in Fig. 1). In this way both the lepton flavour and charge independent results as well as OS (electron) dominance over SS (muon) signals can be recovered. It happens for θ_{13} and ϕ_{13} values which satisfies Eq. (30).

Let us remark that naive usage of NWA would not capture dependence on CP phases $\phi_{2,3}$ at all, neither interference between diagrams with different N_a correctly, what will result in wrong $\theta_{12,13}$ dependence, nor contributions from diagram with crossed lepton lines in the case of same-flavour signature. This should be kept in mind when confronting refined models with data.

3.4. Dependence on heavy neutrino mass splitting $\Delta M = M_{N_2} - M_{N_1}$

Here we want to show some general dependence of the cross section on mass difference between N_2 and N_1. For simplicity it is assumed that mass of the first and third heavy neutrino are fixed to 1 TeV.

Let us note first that σ decreases when $M_{N_2} \to M_{W_2}$, see Fig. 7. It is a consequence of decreasing branching ratio, see (36) in Appendix A. This effect is substantial; the cross section can be suppressed by a factor of 2 for considered masses.

When $M_{N_2} > M_{W_2}$ then the decay $W_2 \to lN_2$ is kinematically forbidden. It means that N_2 cannot be on-shell hence the contribution from such a diagram is very small because it is not enhanced by the N_2-resonance, cross section starts to be flat in Fig. 7.

The second effect worth mentioning, is constructive or destructive interference between diagrams with N_1 and N_2 when

M_{N_2} goes across $M_{N_{1,3}}$. Due to very small width of N_a, $\Gamma(N_a) \sim 10^{-3}$ GeV, the interference effect is visible only in the 'very degenerate' case i.e. when mass difference $|M_{N_{1,3}} - M_{N_2}|$ between heavy neutrinos is smaller than about 0.005 GeV. Let us stress that due to these interference effects cross section σ can be suppressed by an additional factor of 0.5 or increased by 1.5, see Fig. 7. Hence, very small mass splitting between heavy neutrinos can be a source of additional suppression/enhancement of the discussed cross section. However, as a width is very small, it might be difficult to discover such effects experimentally (energy resolution).

4. Summary and outlook

We have revisited production of two light charged leptons and two jets in pp collision in the context of the genuine MLRSM with $g_L = g_R$. Taking into account details on the neutrino mass matrix parameters, interesting conclusions can be derived. Recent CMS data showed that:

(i) there is an excess in the total $pp \to eejj$ cross section at about $M_{W_2} \approx 2.2$ TeV;
(ii) there is a suppression of same-sign electron pairs with respect to opposite-sign pairs in $pp \to eejj$ events;
(iii) there is a suppression of muon pairs with respect to electron pair in $pp \to lljj$ events.

These facts cannot be explained within the MLRSM with $g_L = g_R$, degenerate heavy neutrino mass spectrum, and no neutrino mixings in K_R.

However, we have shown that all the issues (i)–(iii) listed above can be reconciled with the $g_L = g_R$ MLRSM, if non-degenerate heavy neutrino mass spectrum, neutrino mixings in K_R and CP phases are taken into account.

We also conclude that it is worth to undertake more careful analyses of the neutrino sector when exclusion plots are considered, otherwise too strong limits can be inferred from a simplified scenario (in this case assuming real neutrino mixing matrix elements with degenerate heavy neutrinos). An example is specific, but conclusions which we can derive are more general as heavy neutrinos are present within many BSM models.

In our analyses we kept M_{W_2} fixed at the CMS value 2.2 TeV, however, in the light of leptogenesis [49], it would be interesting to check if it is possible to reproduce CMS data with M_{W_2} shifted up to about 3 TeV by relaxing $M_{W_2} - M_N$ mass relation ($M_N = M_{W_2}/2$) and exploring wide space of heavy neutrino mixing angles, phases and masses (not necessarily of the degenerate nature), similarly as we have made in this work. It will be worthwhile to study that issue when better statistics is available.

As an outlook, we would like to check more carefully contributions from the scalar sector in the MLRSM and confront our scenarios which include heavy neutrino mixing parameters and CP phases with other delicate low-energy data as neutrinoless double beta decay, just to mention [11,32,50–53].

Acknowledgements

Appendix A

We collect here some basic formulas useful in calculations and basic estimations.

- Quark gauge interactions [38]:

$$\mathcal{L} \supset \frac{g_R}{\sqrt{2}} \bar{q}_\alpha \left(U_{CKM}^{R\,\dagger} \right)_{\alpha\beta} P_- \gamma^\mu q_\beta W_{2\mu}^-$$
$$+ \frac{g_R}{\sqrt{2}} \bar{q}_\beta \gamma^\mu P_+ \left(U_{CKM}^R \right)_{\beta\alpha} q_\alpha W_{2\mu}^+. \tag{31}$$

- 2-body decay contributions to BR were calculated in FEYN-RULES. We treat leptons $l_i^\pm$ as massless:

$$\Gamma(W_2^+ \to l_i^+ N_a) = \frac{g_L^2 M_{W_2}}{96\pi} |(K_R^\dagger)_{ia}|^2 F_W(x_a), \tag{32}$$

where $x_a = M_{N_a}^2 / M_{W_2}^2$ and $F_W(x) = (2 - 3x + x^3)\theta(1 - x)$. θ function in the definition of F_W takes care of kinematic constraints for the decays. Because even for top quark the ratio $M_{q_\alpha}^2/M_{W_2}^2$ is of the order of 10^{-2} one can treat quarks in the final states as massless. Hence, taking into account $F_W(0) = 2$ and summing over colours:

$$\Gamma(W_2^+ \to q_\alpha \bar{q}_\beta) = \frac{g_L^2 M_{W_2}}{16\pi} |(U_{CKM}^{R\,\dagger})_{\alpha\beta}|^2, \tag{33}$$

$$\Gamma(W_2^- \to \bar{q}_\alpha q_\beta) = \frac{g_L^2 M_{W_2}}{16\pi} |(U_{CKM}^{R\,T})_{\alpha\beta}|^2. \tag{34}$$

That yields the total width of $W_2^\pm$

$$\Gamma(W_2^\pm) = \frac{g_L^2 M_{W_2}}{96\pi} \left[\sum_a F_W(x_a) + 18 \right] \tag{35}$$

and branching ratio for $W_2^\pm \to l_i^\pm N_a$:

$$\mathrm{BR}(W_2^\pm \to l_i^\pm N_a) = |(K_R^\dagger)_{ia}|^2 \frac{F_W(x_a)}{18 + \sum_c F_W(x_c)}. \tag{36}$$

That formula gives very good estimate of branching ratio; e.g. for $x_1 = 1/4$, $x_{2,3} > 1$ and $K_R = 1$ one gets $\mathrm{BR}(\ldots)/\mathrm{BR}(\ldots)_{\mathrm{MadGraph}} \approx 0.0657/0.0659 \approx 0.997$, and similarly for $x_{1,2,3} = 1/4$: $\mathrm{BR}(\ldots)/\mathrm{BR}(\ldots)_{\mathrm{MadGraph}} \approx 0.0581/0.0582 \approx 0.998$.

The branching ratio for decay to quarks is:

$$\mathrm{BR}(W_2^\pm \to q_\alpha \bar{q}_\beta) = |(U_{CKM}^R)_{\beta\alpha}|^2$$
$$\times \frac{6}{18 + \sum_c F_W(x_c)}. \tag{37}$$

References

[1] V. Khachatryan, et al., CMS Collaboration, arXiv:1407.3683 [hep-ex].
[2] F.F. Deppisch, T.E. Gonzalo, S. Patra, N. Sahu, U. Sarkar, Phys. Rev. D 90 (2014) 053014, arXiv:1407.5384 [hep-ph].
[3] M. Heikinheimo, M. Raidal, C. Spethmann, Eur. Phys. J. C 74 (2014) 3107, arXiv:1407.6908 [hep-ph].
[4] F.F. Deppisch, T.E. Gonzalo, S. Patra, N. Sahu, U. Sarkar, Phys. Rev. D 91 (2015) 015018, arXiv:1410.6427 [hep-ph].
[5] J.A. Aguilar-Saavedra, F.R. Joaquim, Phys. Rev. D 90 (2014) 115010, arXiv:1408.2456 [hep-ph].
[6] R. Mohapatra, J.C. Pati, Phys. Rev. D 11 (1975) 2558.
[7] G. Senjanovic, R.N. Mohapatra, Phys. Rev. D 12 (1975) 1502.
[8] R.N. Mohapatra, G. Senjanovic, Phys. Rev. D 23 (1981) 165.
[9] V. Khachatryan, et al., CMS Collaboration, arXiv:1501.05566 [hep-ex].

[10] A. Maiezza, M. Nemevsek, F. Nesti, G. Senjanovic, Phys. Rev. D 82 (2010) 055022, arXiv:1005.5160 [hep-ph].

[11] V. Tello, M. Nemevsek, F. Nesti, G. Senjanovic, F. Vissani, Phys. Rev. Lett. 106 (2011) 151801, arXiv:1011.3522 [hep-ph].

[12] M. Nemevsek, F. Nesti, G. Senjanovic, Y. Zhang, Phys. Rev. D 83 (2011) 115014, arXiv:1103.1627 [hep-ph].

[13] M. Nemevsek, G. Senjanovic, Y. Zhang, J. Cosmol. Astropart. Phys. 1207 (2012) 006, arXiv:1205.0844 [hep-ph].

[14] S.P. Das, F.F. Deppisch, O. Kittel, J.W.F. Valle, Phys. Rev. D 86 (2012) 055006, arXiv:1206.0256 [hep-ph].

[15] J. Adelman, J. Ferrando, C.D. White, J. High Energy Phys. 1302 (2013) 091, arXiv: 1206.5731 [hep-ph].

[16] M. Nemevsek, G. Senjanovic, V. Tello, Phys. Rev. Lett. 110 (2013) 151802, arXiv: 1211.2837 [hep-ph].

[17] C.H. Lee, P.S. Bhupal Dev, R.N. Mohapatra, Phys. Rev. D 88 (2013) 093010, arXiv:1309.0774 [hep-ph].

[18] R.N. Mohapatra, Y. Zhang, Phys. Rev. D 89 (2014) 055001, arXiv:1401.0018 [hep-ph].

[19] C.Y. Chen, P.S.B. Dev, R.N. Mohapatra, Phys. Rev. D 88 (2013) 033014, arXiv: 1306.2342 [hep-ph].

[20] S. Bertolini, A. Maiezza, F. Nesti, Phys. Rev. D 89 (9) (2014) 095028, arXiv: 1403.7112 [hep-ph].

[21] A. Maiezza, M. Nemevšek, Phys. Rev. D 90 (9) (2014) 095002, arXiv:1407.3678 [hep-ph].

[22] J.C. Vasquez, arXiv:1411.5824 [hep-ph];
J.C. Vasquez, arXiv:1504.05220 [hep-ph].

[23] U. Aydemir, D. Minic, C. Sun, T. Takeuchi, Phys. Rev. D 91 (2015) 045020, arXiv: 1409.7574 [hep-ph].

[24] F. Staub, arXiv:1409.7182 [hep-ph].

[25] B. Dutta, R. Eusebi, Y. Gao, T. Ghosh, T. Kamon, Phys. Rev. D 90 (2014) 055015, arXiv:1404.0685 [hep-ph].

[26] N. Mahajan, Phys. Rev. D 90 (2014) 035015, arXiv:1406.2606 [hep-ph].

[27] F.J. de Anda, Mod. Phys. Lett. A 30 (2015) 1550063, arXiv:1403.4902 [hep-ph].

[28] G. Senjanovic, V. Tello, Phys. Rev. Lett. 114 (2015) 071801, arXiv:1408.3835 [hep-ph].

[29] A. Maiezza, M. Nemevsek, F. Nesti, arXiv:1503.06834 [hep-ph].

[30] P.S. Bhupal Dev, C.H. Lee, R.N. Mohapatra, arXiv:1503.04970 [hep-ph].

[31] G. Senjanovic, V. Tello, arXiv:1502.05704 [hep-ph].

[32] G. Bambhaniya, J. Chakrabortty, J. Gluza, M. Kordiaczyńska, R. Szafron, J. High Energy Phys. 1405 (2014) 033, arXiv:1311.4144 [hep-ph];
G. Bambhaniya, J. Chakrabortty, J. Gluza, T. Jeliński, M. Kordiaczyńska, Phys. Rev. D 90 (2014) 095003, arXiv:1408.0774 [hep-ph];
G. Bambhaniya, J. Chakrabortty, J. Gluza, T. Jeliński, R. Szafron, arXiv:1504. 03999 [hep-ph].

[33] R.N. Mohapatra, Unification and Supersymmetry: The Frontiers of Quark – Lepton Physics, Springer, New York, 2003.

[34] Neutrino web page, http://www.nu.to.infn.it/.

[35] C. Giunti, C.W. Kim, Fundamentals of Neutrino Physics and Astrophysics, OUP, Oxford, 2007.

[36] W.Y. Keung, G. Senjanovic, Phys. Rev. Lett. 50 (1983) 1427.

[37] W. Buchmüller, C. Greub, P. Minkowski, Phys. Lett. B 267 (1991) 395;
J. Gluza, Acta Phys. Pol. B 33 (2002) 1735;
A. Pilaftsis, Phys. Rev. Lett. 95 (2005) 081602;
Z.-z. Xing, Prog. Theor. Phys. Suppl. 180 (2009) 112;
X.-G. He, S. Oh, J. Tandean, C.-C. Wen, Phys. Rev. D 80 (2009) 073012;
A. Ibarra, E. Molinaro, S.T. Petcov, J. High Energy Phys. 1009 (2010) 108;
R. Adhikari, A. Raychaudhuri, Phys. Rev. D 84 (2011) 033002;
M. Mitra, G. Senjanovic, F. Vissani, Nucl. Phys. B 856 (2012) 26.

[38] J. Gluza, M. Zrałek, Phys. Rev. D 48 (1993) 5093;
P. Duka, J. Gluza, M. Zrałek, Ann. Phys. 280 (2000) 336, arXiv:hep-ph/9910279.

[39] S.M. Bilenky, S.T. Petcov, Rev. Mod. Phys. 59 (1987) 671;
S.M. Bilenky, S.T. Petcov, Rev. Mod. Phys. 60 (1988) 575(E);
S.M. Bilenky, S.T. Petcov, Rev. Mod. Phys. 61 (1989) 169(E).

[40] B. Kayser, in: C. Jarlskog (Ed.), CP Violation, World Scientific, Singapore, 1989.

[41] J. Gluza, M. Zrałek, Phys. Rev. D 51 (1995) 4707;
J. Gluza, M. Zrałek, Phys. Lett. B 362 (1995) 148;
J. Gluza, M. Zrałek, Phys. Lett. B 372 (1996) 259;
J. Gluza, J. Maalampi, M. Raidal, M. Zrałek, Phys. Lett. B 407 (1997) 45;
J. Gluza, Phys. Lett. B 403 (1997) 304.

[42] J. Alwall, M. Herquet, F. Maltoni, O. Mattelaer, T. Stelzer, J. High Energy Phys. 1106 (2011) 128, arXiv:1106.0522 [hep-ph].

[43] N.D. Christensen, C. Duhr, Comput. Phys. Commun. 180 (2009) 1614, arXiv: 0806.4194 [hep-ph].

[44] C. Degrande, C. Duhr, B. Fuks, D. Grellscheid, O. Mattelaer, T. Reiter, Comput. Phys. Commun. 183 (2012) 1201, arXiv:1108.2040 [hep-ph].

[45] G. Aad, et al., ATLAS Collaboration, Phys. Rev. D 91 (2015) 052007, arXiv: 1407.1376 [hep-ex].

[46] Z. Maki, M. Nakagawa, S. Sakata, Prog. Theor. Phys. 28 (1962) 870;
B. Pontecorvo, Zh. Eksp. Teor. Fiz. 53 (1967) 1717; Sov. Phys. JETP 26 (1968) 984;
B. Dziewit, S. Zając, M. Zrałek, Acta Phys. Pol. B 42 (2011) 2509, arXiv:1204. 3665 [hep-ph];
K.A. Olive, et al., Particle Data Group Collaboration, Chin. Phys. C 38 (2014) 090001.

[47] F. del Aguila, M. Zrałek, Nucl. Phys. B 447 (1995) 211.

[48] A. Ferroglia, C. Greub, A. Sirlin, Z. Zhang, Phys. Rev. D 88 (2013) 033012, arXiv: 1307.6900.

[49] M. Dhuria, C. Hati, R. Rangarajan, U. Sarkar, Phys. Rev. D 91 (2015) 055010, arXiv:1501.04815 [hep-ph];
M. Dhuria, C. Hati, R. Rangarajan, U. Sarkar, arXiv:1502.01695 [hep-ph];
M. Dhuria, C. Hati, R. Rangarajan, U. Sarkar, arXiv:1503.07198 [hep-ph].

[50] J. Chakrabortty, J. Gluza, R. Sevillano, R. Szafron, J. High Energy Phys. 1207 (2012) 038, arXiv:1204.0736 [hep-ph].

[51] J. Chakrabortty, H.Z. Devi, S. Goswami, S. Patra, J. High Energy Phys. 1208 (2012) 008, arXiv:1204.2527 [hep-ph].

[52] W. Rodejohann, J. Phys. G 39 (2012) 124008, arXiv:1206.2560 [hep-ph].

[53] P.S. Bhupal Dev, S. Goswami, M. Mitra, W. Rodejohann, Phys. Rev. D 88 (2013) 091301, arXiv:1305.0056 [hep-ph].